Acta Crystallographica Section F
Structural Biology and Crystallization Communications
ISSN 1744-3091

Crystallization and molecular-replacement solution of a diagnostic fluorescent dye in complex with a specific Fab fragment

Roman C. Hillig,[a]* Siegfried Baesler,[a] Stefanie Urlinger,[b] Yvonne Stark,[b] Susanne Bauer,[b] Volker Badock,[a] Martina Huber,[a] Inke Bahr,[a] Michael Schirner[a] and Kai Licha[a]

[a]Bayer Schering Pharma AG, Research Laboratories, D-13342 Berlin, Germany, and [b]MorMorphosys AG, Lena-Christ-Strasse 48, D-82152 Martinsried, Germany

Correspondence e-mail: roman.hillig@schering.de

Received 22 December 2006
Accepted 3 February 2007

Tetrasulfocyanine (TSC) has been described as a fluorescent probe for tumour imaging. The complex of TSC and the Fab antibody fragment MOR03268 has been crystallized in three different crystal forms. MOR03268 was identified from the HuCAL GOLD library and further optimized to bind TSC with high affinity (K_d = 0.6 n*M*). For two of the three crystal forms (forms 1 and 2), data sets could be collected to 2.8 and 2.85 Å resolution, respectively. Form 1 belongs to space group *I*222, with unit-cell parameters $a = 72$, $b = 99$, $c = 154$ Å. Form 2 belongs to space group $P4_32_12$, with unit-cell parameters $a = b = 77$, $c = 379$ Å. Form 3 only diffracted to 8 Å and was not analyzed further. Molecular-replacement solutions for forms 1 and 2 were found and rebuilding and refinement is in progress. Form 1 contains one Fab molecule per asymmetric unit, while form 2 harbours two. Judging from the green colour of the crystals, both forms contain the Fab molecule bound to the green TSC dye and in both the hydrolysis-sensitive dye molecule is protected from degradation for several weeks to months. The structures should reveal the molecular basis of the high-affinity recognition of TSC by the Fab molecule MOR03268.

1. Introduction

The near-infrared fluorescent dye tetrasulfocyanine (TSC) is currently under evaluation as a nonspecific diagnostic agent in optical imaging (Perlitz *et al.*, 2005). A general means of increasing the molecular specificity of imaging agents is to attach them to target-directed vehicles (peptides, antibodies) or to follow the concept of pre-targeting using bivalent antibodies, as successfully demonstrated for radioimmunotherapy (Gruaz-Guyon *et al.*, 2005). For the latter purpose, we developed fully human Fab antibody fragments which specifically recognize TSC and thus may be used as part of bispecific antibodies to target this dye to cellular targets of choice. Here, we present the crystallization of MOR03268, a phage-display-derived Fab molecule which recognizes TSC with a K_d of 0.6 n*M* as determined by solution equilibrium titration (Haenel *et al.*, 2005). Crystals grew in the presence of the dye and their dark green colour suggests that the dye is bound to the Fab in the crystal.

2. Methods

2.1. Dye synthesis and protein production

The indotricarbocyanine dye tetrasulfocyanine (TSC) and its conjugates to albumin and transferrin were synthesized as described previously (Perlitz *et al.*, 2005; Licha & Perlitz, 2004). The antibody MOR03268 was developed to specifically bind TSC using phage display and the HuCAL GOLD library (Kretzschmar & von Rüden, 2001), in which all six complementarity-determining regions (CDRs) of Fab antibody fragments are diversified using trinucleotide mutagenesis (Virnekäs *et al.*, 1994). Details will be published elsewhere. The antibody fragment was cloned into the pMORPHX9_MH expression vector (Rauchenberger *et al.*, 2003), expressed in *Escherichia coli* and purified *via* nickel-affinity chromatography (Ni–NTA His-Bind Superflow Sepharose from Novagen; elution buffer 20 m*M* sodium phosphate, 500 m*M* NaCl, 250 m*M* imidazole pH 7.4).

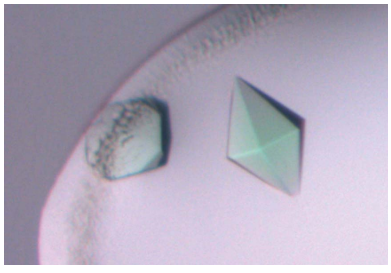

© 2007 International Union of Crystallography
All rights reserved

Table 1
Data-collection statistics for crystals of the MOR03268–TSC complex.

Values in parentheses are for the highest resolution shell.

Data set	1	2	3	4
Crystal form	Form 1 (low resolution)	Form 1 (high resolution)	Form 2 (low resolution)	Form 2 (high resolution)
Beamline	X06SA (SLS)	BL1 (BESSY)	BL1 (BESSY)	X06SA (SLS)
Wavelength (Å)	0.97630	0.9184	0.9184	0.9999
Temperature (K)	100	100	100	100
Crystal dimensions (µm)	400 × 25 × 25	300 × 40 × 40	100 × 100 × 40	100 × 100 × 40
Mosaicity (°)	0.7	0.6	0.9	0.3
$\Delta\varphi$ per image (°)	1	1	1	1
Total φ range (°)	120	229	88	77
Crystal-to-detector distance (mm)	200	200	250	220
Space group	*I*222	*I*222	$P4_32_12$	$P4_32_12$
Unit-cell parameters (Å)	a = 71.6, b = 99.3, c = 154.3	a = 71.9, b = 98.5, c = 153.8	$a = b$ = 77.0, c = 379.2	$a = b$ = 77.0, c = 379.1
Resolution range (Å)	49.6–3.0 (3.07–3.00)	41.7–2.8 (2.85–2.80)	48.9–3.2 (3.26–3.20)	48.9–2.85 (2.90–2.85)
Unique reflections	10804 (517)	13432 (534)	19385 (856)	27756 (1058)
Multiplicity	4.6 (2.7)	5.5 (3.4)	5.5 (4.2)	5.7 (3.9)
Completeness (%)	95.9 (75.4†)	97.6 (79.8†)	97.3 (82.5)	98.7 (78.8)
I/σ	7.4 (1.5)	17.1 (2.2)	10.7 (1.9)	15.6 (3.5)
Wilson B factor‡ (Å^2)	57.4	61.5	75.6	72.2
$R_{\rm sym}$	0.144 (0.440)	0.097 (0.554)	0.141 (0.513)	0.100 (0.392)

† The highest resolution shell was incomplete owing to anisotropic diffraction of the needle-shaped crystal form 1. ‡ From *TRUNCATE* (Collaborative Computational Project, Number 4, 1994).

The buffer was exchanged to PBS (136 m*M* NaCl, 2.7 m*M* KCl, 8.1 m*M* Na_2HPO_4, 1.5 m*M* KH_2PO_4 pH 7.3) using a PD10 desalting column and the sample was sterile filtered (0.2 µm), frozen and stored at 193 K.

For all crystallization trials, the sample was thawed, the buffer was exchanged to 20 m*M* Tris–HCl pH 7.5, 50 m*M* NaCl using dialysis and the sample was concentrated to 11.8 mg ml^{-1} (Amicon Ultra-4 Centrifuge Device, 10 kDa cutoff). The homogeneity of the purified Fab sample was confirmed by analytical gel filtration (Superdex S200, running buffer 20 m*M* Tris–HCl pH 7.5, 50 m*M* NaCl) and dynamic light scattering (Dyna Pro MS800, Protein Solutions; in gel-filtration running buffer at concentrations for crystallization; 20 measurements were averaged with acquisition times of 5 s). The identity of the antibody was confirmed by measuring the molecular weight using LC-ESI-MS (Applied Biosystems QSTAR XL quadrupole TOF mass spectrometer connected to a Dionex Ultimate HPLC system using a 200 µm ID monolithic column).

2.2. Crystallization

Crystallization experiments were carried out using vapour-diffusion methods (sitting drop in Greiner 96-well plates and hanging

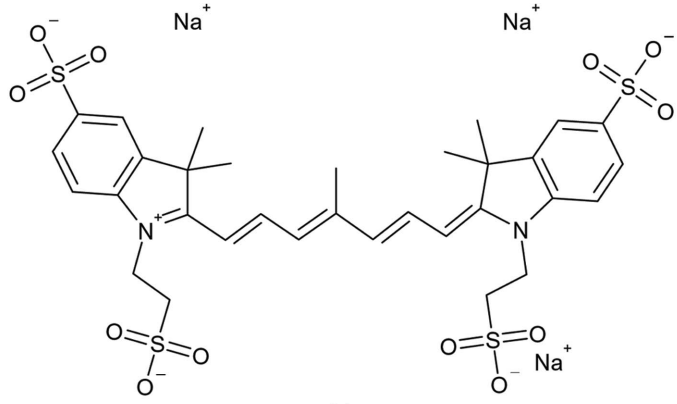

(*a*)

Heavy chain: VH-CH1 MOR03268 with **myc-His tag**

QVQLVQSGAEVKKPGSSVKVSCKASGGTFSNYAINWVRQAPGQGLEWMGNIEPYFGTANYAQKFQGRVTITA
DESTSTAYMELSSLRSEDTAVYYCARYFMSYKHLSDYWGQGTLVTVSSASTKGPSVFPLAPSSKSTSGGTAA
LGCLVKDYFPEPVTVSWNSGALTSGVHTFPAVLQSSGLYSLSSVVTVPSSSLGTQTYICNVNHKPSNTKVDK
KVEPKSEF**EQKLISEEDLNGAPHHHHHH**

(*b*)

Light chain: VL-CL MOR03268

DIALTQPASVSGSPGQSITISCTGTSSDVGSNNYVSWYQQHPGKAPKLMIYGGSNRPSGVSNRFSGSKSGNT
ASLTISGLQAEDEADYYCRSWDSNLSYSVFGGGTKLTVLGQPKAAPSVTLFPPSSEELQANKATLVCLISDF
YPGAVTVAWKADSSPVKAGVETTTPSKQSNNKYAASSYLSLTPEQWKSHRSYSCQVTHEGSTVEKTVAPTEA

(*c*)

Figure 1
Structure of TSC and sequence of the Fab molecule MOR03268. (*a*) Structure of the fluorescent dye tetrasulfocyanine (TSC). (*b*) Amino-acid sequence of the heavy chain of the Fab molecule MOR03268. The sequence of the C-terminal myc-His_6 tag is shown in bold. (*c*) Sequence of the light chain of MOR03268.

drop in Linbro 24-well plates). The complex of the Fab molecule MOR03268 and TSC was formed by the addition of a TSC stock solution (12 m*M* in water), resulting in final concentrations of 1 m*M* TSC and 0.2 m*M* (10 mg ml^{-1}) protein. Drops consisted of 1 µl protein/dye solution and 1 µl reservoir solution (the reservoir was 1 ml for 24-well plates and 100 µl for 96-well plates). All experiments were stored at 293 K. Crystals of three different crystal forms grew from reservoir solutions containing 1.6–2.6 *M* ammonium sulfate (AS) as precipitant, 5% PEG 400 as an additive and 100 m*M* buffer (sodium citrate pH 4.0 or MES pH 6.0).

Crystals of the rod-shaped crystal form 1 grew from 2.3 *M* AS pH 4.0 and were frozen using cryobuffer *A* (2.4 *M* AS, 0.1 *M* sodium citrate pH 4.0, 15% glycerol) by stepwise exchange of the complete drop for cryobuffer over 10 min. The more compact crystal form 2 grew from 2.6–2.7 *M* AS pH 4.0 and was flash-frozen after quick exposure to cryobuffer *B* (2.8 *M* AS, 0.1 *M* sodium citrate pH 4.0, 5% PEG 400, 10% glycerol). The third crystal form (hexagonal bipyramids) grew from 1.6 *M* AS pH 6.0 and was frozen after exchange of the complete drop for cryobuffer *C* (1.8 *M* AS, 0.1 *M* MES pH 6.0, 5% PEG 400, 15% glycerol).

2.3. Data collection and molecular replacement

An initial data set for crystal form 1 was collected at the Swiss Light Source (SLS), Villigen, Switzerland and was used to solve the structure by molecular replacement and to start rebuilding and refinement (see below). A second higher resolution data set collected at the BESSY synchrotron in Berlin was used to continue refinement. For further details, see Table 1. For form 2, an initial data set collected at BESSY enabled structure determination *via* molecular replacement. A second higher resolution data set was subsequently collected at the SLS and used for refinement. Crystals of form 3 only diffracted to 8 Å at the SLS and a full data set was not collected. All data sets were collected using a MAR CCD detector, processed using *HKL-*

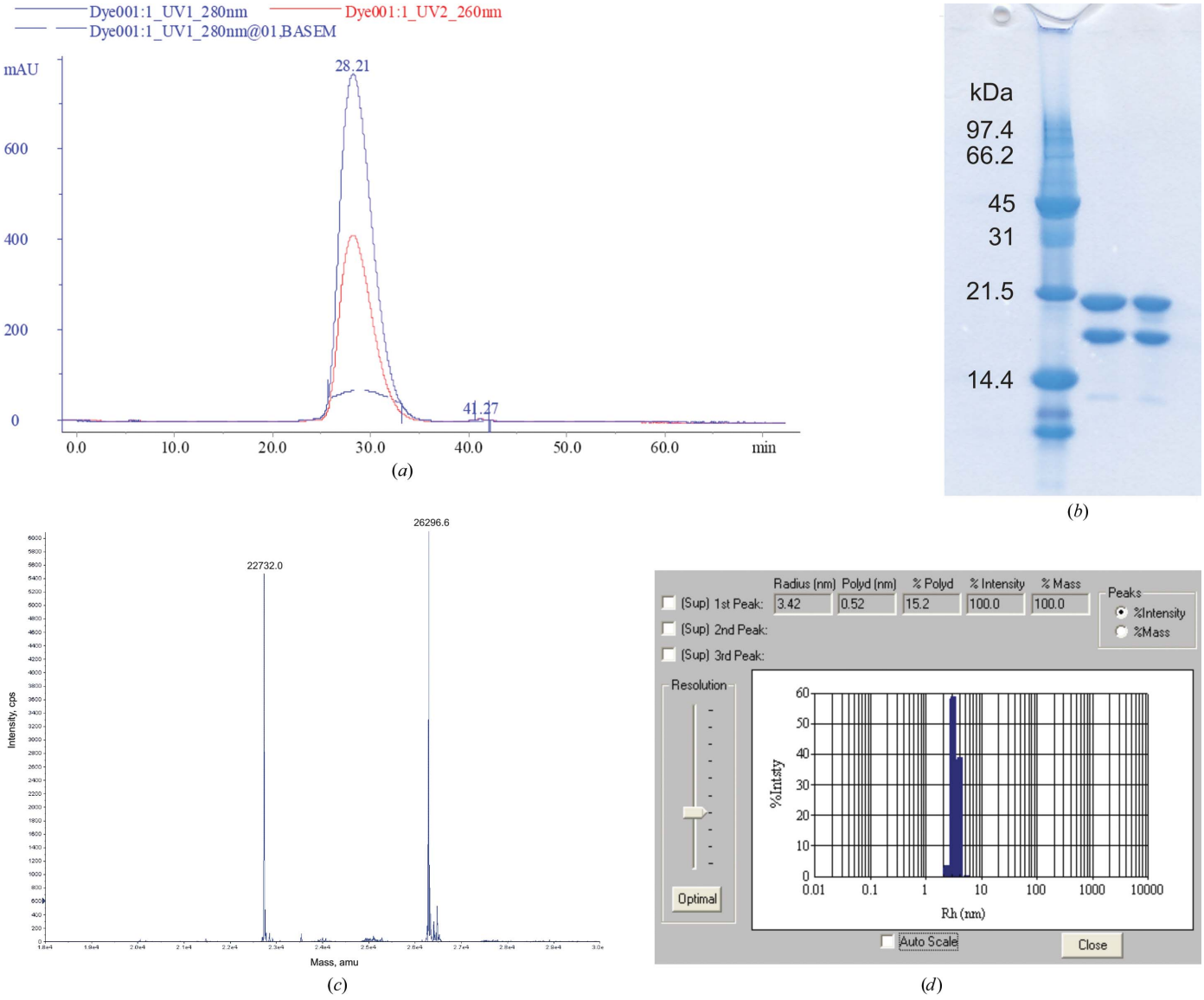

Figure 2
Characterization of the purified Fab molecule MOR03268. (*a*) Analytical HPLC gel-filtration elution diagram (Sephadex G75) confirming the homogeneity of the purified sample after storage at 193 K and re-thawing. (*b*) PAGE analysis (non-reducing conditions) showing two bands for the heavy and light chain of MOR03268. Both sample lanes were loaded with 4.8 µg Fab. (*c*) Deconvoluted ESI–MS spectrum, confirming the exact molecular mass of the HC and LC. (*d*) Regulation histogram of MOR03268 at 1 mg ml^{-1} indicating a homogeneous monomeric species (hydrodynamic radius 3.4 nm; monomodal polydispersity 15%).

2000 (Otwinowski & Minor, 1997) and analysed using the programs *MATTHEWS_COEF* and *TRUNCATE* from the *CCP*4 suite (Collaborative Computational Project, Number 4, 1994).

Crystal form 1 was processed in space group *I*222 and had a Matthews coefficient V_M of 2.8 Å^3 Da^{-1} (solvent content 0.56) assuming the presence of one Fab molecule per asymmetric unit (Matthews, 1968). Successful molecular replacement [carried out with *MOLREP* (Vagin & Teplyakov, 1997) from the *CCP*4 suite (Collaborative Computational Project, Number 4, 1994)] confirmed that *I*222 (and not $I2_12_12_1$) was the correct space group. Molecular-replacement searches were carried out separately for both the heavy chain (HC) and the light chain (LC), using as search models the ten closest relatives (at the sequence level) for each chain from the Protein Data Bank (PDB; Berman *et al.*, 2000). Sequence identities were 0.76–0.83 for the HC and 0.80–0.82 for the LC. A solution for the HC was found using the closest HC relative (PDB code 1vge, residues H1–H225) in space group *I*222 (correlation coefficient 0.312 and *R* factor 0.569). The best solution in the wrong space group $I2_12_12_1$ featured a correlation coefficient (CC) of 0.25 and an *R* factor of 0.595; the second best search model (HC of 1axs) in the correct space group *I*222 gave a CC of 0.229 and an *R* factor of 0.600. With the HC solution fixed, molecular replacement using the ten closest LC relatives was not successful. The search was continued separately with smaller fragments of the LC, namely the constant domain (C_L) and the variable domain (V_L). A solution was found only for C_L, using C_L of 1vge (residues L109–L214) as the search model (CC 0.389 and *R* factor 0.576 with the HC solution fixed). Refinement of this partial model (HC and C_L from 1vge, sequence mutated to that of MOR03268) was started using *CNX* (Accelrys Inc., San Diego), the commercial version of *CNS* (Brünger *et al.*, 1998).

A solution for the missing V_L domain was finally found by manually positioning the corresponding region of 1vge (residues L1–L108) by superimposition of 1vge on the partial molecular-replacement solution followed by rigid-body refinement of this V_L orientation with *CNX*. After one round of rebuilding (*Quanta*; Accelrys Inc., San Diego) and refinement, regions of V_L which were still very poorly defined were deleted and partly replaced by sections of V_L of PDB entry 1a9j (residues L3–L112, sequence mutated to that of MOR03268 using *MOLREP*). The latter had been positioned manually in the same way as described above for V_L of 1vge. V_L of entry 1a8j was identified as the closest sequence relative to this region of MOR03268 in the PDB. Rebuilding and refinement was started with data set 1, continued with data set 2 (Table 1) and is currently being completed. Difference density maps allowed the placement of the ligand (data not shown).

Data for crystal form 2 were first processed in space group *P*4. Analysis with *XPREP* (Bruker AXS, Madison) indicated space group $P4_12_12$ or $P4_32_12$, both with a Matthews coefficient V_M of 2.9 Å^3 Da^{-1} (solvent content 0.57) assuming two Fab molecules per asymmetric unit. Molecular replacement was carried out in parallel in both space groups using *MOLREP* with the preliminarily refined structure of crystal form 1 as the search model. This identified $P4_32_12$ as the correct space group (best solution after placing two search molecules, *R* 0.555, CC 0.325; second best solution, *R* 0.608, CC 0.217; best solution in $P4_12_12$, *R* 0.583, CC 0.276; second best solution, *R* 0.603, CC 0.214). Initial refinement in $P4_32_12$ using *CNX* confirmed this

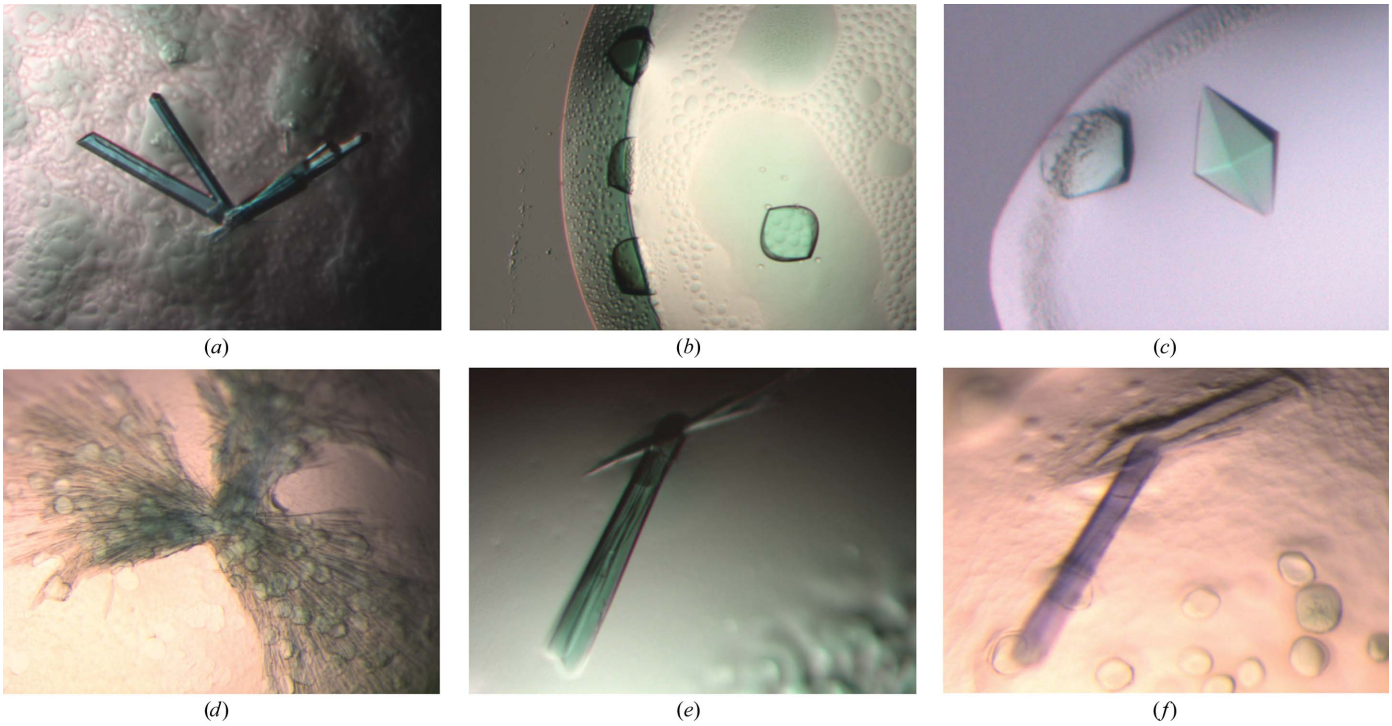

Figure 3
Crystallization of the MOR03268–TSC complex. (*a*) Rod-shaped crystals of crystal form 1. Individual crystals grew to a length of about 400–800 µm and a thickness of up to 40 µm. (*b*) Onion-shaped crystals of form 2, growing from a drop showing strong phase separation. Their dimensions are about 100 × 100 × 40 µm. (*c*) Hexagonal bipyramids of crystal form 3 (length about 120 µm, width 60 µm). (*d*) A drop that initially contained only needle-shaped crystals of form 1, which grew as a bundle. After storage at 293 K for about a year, re-crystallization has taken place and crystals of form 2 have appeared. (*e*, *f*) After storage for ten months, this crystal of form 1 has lost its original green colour (shown in *e*) and has adopted a purple colour (*f*). In addition, crystals of form 2 have appeared in the background. The colour change to purple most likely indicates that the dye has been degraded in its central linker region, as the expected degradation product would be purple. Interestingly, this partially degraded ligand must still be bound to the Fab molecule, otherwise the crystals would have lost all colour.

choice as it showed density for the ligand, which was not itself included in the search model. Refinement was started with data set 3 and was subsequently continued with the higher resolution data set 4 (Table 1). Refinement and analysis of both structures is ongoing and will be published elsewhere.

3. Results and discussion

3.1. Protein production and characterization

The Fab antibody fragment MOR03268 was identified *via* phage display from the HuCAL GOLD antibody library (for a review, see Ostendorp *et al.*, 2004) and was optimized by one round of maturation to bind TSC with high affinity. Fig. 1 shows the structure of TSC and the amino-acid sequence of the light chain (LC) and heavy chain (HC) of MOR03268. The HC consists of 244 residues (including a C-terminal Myc and His_6 tag which was not cleaved off for crystallization). The LC consists of 216 residues. The Fab molecule was expressed in *E. coli*. Appropriate signal sequences promoted the export of both antibody chains into the bacterial periplasm, where intramolecular disulfide-bond and heterodimer formation take place (for details, see Rauchenberger *et al.*, 2003). After cell lysis, the resulting Fab was purified *via* nickel-affinity chromatography to high homogeneity as shown by size-exclusion chromatography (Fig. 2*a*) and high purity (>95%) as judged from SDS–PAGE analysis (Fig. 2*b*). The exact identity of the purified protein was confirmed by LC-ESI-MS. The expected molecular mass for HC was 22 732.1 and for LC was 26 296.4; the experimentally determined values were 22 732.0 and 26 296.6, respectively (Fig. 2*c*). Dynamic light scattering (Fig. 2*d*) further confirmed that the solution was monodisperse (15–24%), with particles of the expected size indicating a monomeric species at low concentration (1 mg ml^{-1}; hydrodynamic radius 3.4 nm) and a dimeric species at high concentration (11 mg ml^{-1}; hydrodynamic radius 4.2 nm).

3.2. Crystallization

Initial crystals of Fab MOR03268 in complex with TSC were obtained using an in-house PEG/AS grid screen. Small hexagonal bipyramidal crystals only grew after more than five weeks and were found in three conditions which shared 1.4 *M* AS as precipitant and 5% PEG 400 as an additive, while differing in pH and buffer. Well grown bipyramids were only obtained at pH 8.0 (Tris), while crystals at pH 7.3 (HEPES) and 6.0 (MES) grew intertwined. Crystallization drops containing Fab and the green TSC molecule were dark green when the experiment was started. The colour vanished over the course of several days, consistent with the fact that TSC is unstable in water and its degradation products are colourless. All initial crystallization drops were set up in parallel with and without TSC. Crystals were found only in drops supplemented with dye. Moreover, the crystals had clearly a dark green colour, suggesting that they contained Fab bound to TSC and that the binding protected the dye from degradation.

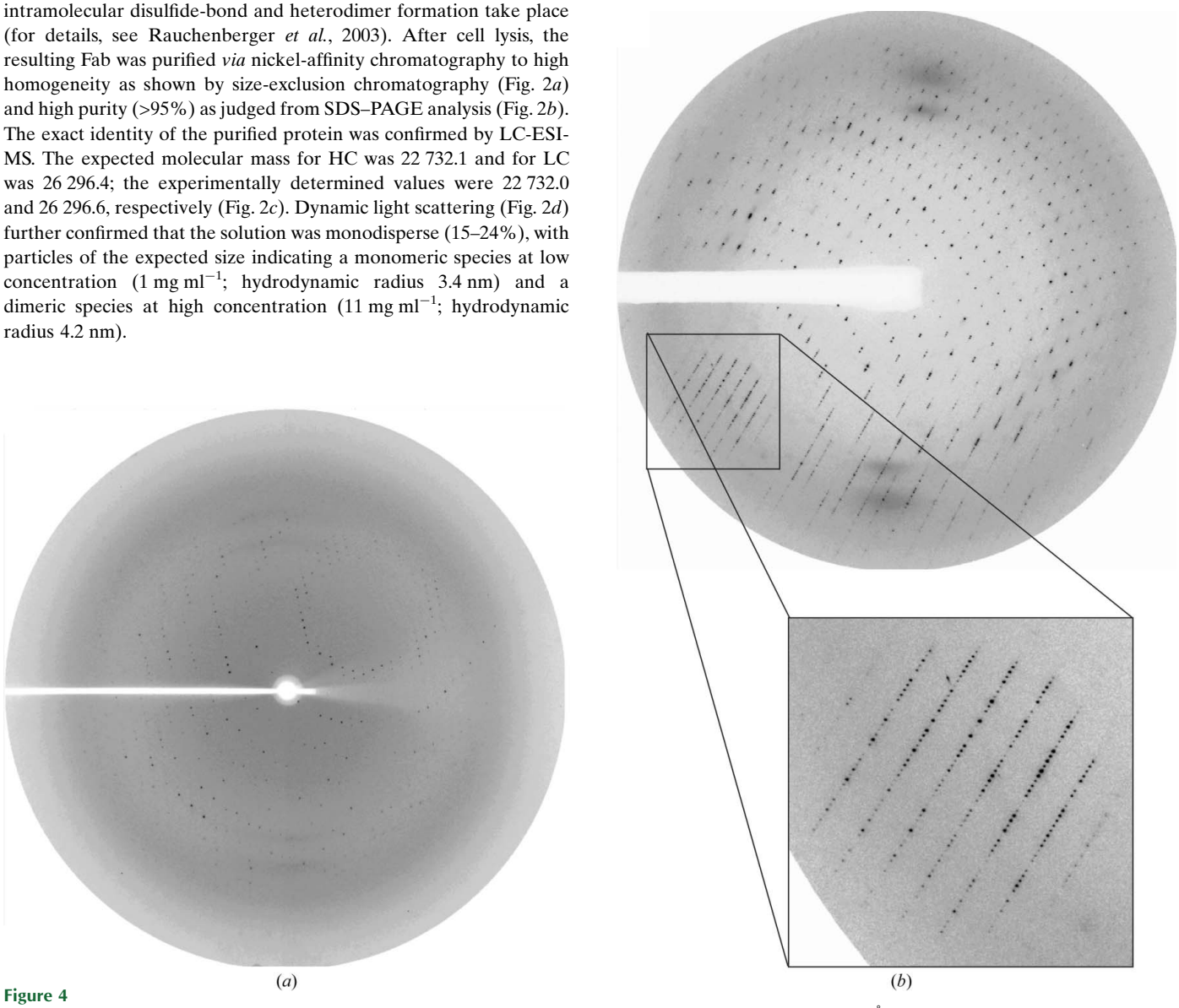

Figure 4
Diffraction images. (*a*) Image of data set 2, crystal form 1, $\Delta\varphi = 1^\circ$, crystal-to-detector distance 200 mm (detector edge 2.5 Å). (*b*) Image of data set 4, crystal form 2, $\Delta\varphi = 1^\circ$, crystal-to-detector distance 220 mm (detector edge 2.8 Å). Despite the very long *c* axis, the reflections could still be resolved.

Despite intensive screening and streak-seeding around these initial conditions, the crystal form could not be reproduced for many months. This was finally overcome by testing a very wide ammonium sulfate–pH screen (0.8–3.2 *M* ammonium sulfate pH 3.0–8.0, modified from Hampton Research) which was set up with 5% PEG 400 as additive in all drops. This approach produced rod-shaped green crystals at 3.2 *M* AS and pH 4.0, a condition distant from that found initially. This new crystal form (termed crystal form 1) grew overnight. An initial data set could be collected from the initial drop (data set 1, Table 1). In order to obtain larger and better diffracting rods, the conditions were optimized. The additive PEG 400 (5%) turned out to be an absolute requirement for crystal growth. Although small crystals of this form grew overnight, larger rods (as shown in Fig. 3*a*) only grew over several weeks. The optimized AS concentration was 2.3 *M* (at pH 4.0).

During the course of refinement, a further crystal form (form 2) was found in two drops containing 2.6 *M* AS as precipitant (pH 4.0). These drops showed strong phase separation and onion-shaped crystals grew in one of the two phases (Fig. 3*b*). As with crystal form 1, these crystals were dark green, indicating the presence of intact TSC. Two crystals from one of these initial drops were used to collect data sets (see below).

The initially observed hexagonal bipyramids (crystal form 3) were later observed again, growing after several weeks at pH 6.0 and at an AS concentration of 1.6 *M* (Fig. 3*c*). However, they could not be grown to a size large enough for sufficient diffraction. Some images were collected to 8 Å at the SLS (data not shown) and suggest that form 3 may belong to a trigonal or hexagonal space group with a *c* axis of about 430 Å. The presence of such a long axis is similar to form 2, where the *c* axis is 379 Å in length (Table 1).

As observed at the very beginning for the bipyramidal crystal form 3, the crystals of the rod-shaped form 1 and the onion-shaped form 2 were dark green in colour and retained this colour over many weeks to months, while the surrounding drop solution lost its dark green colour within 1–2 d. This implied that the TSC dye was protected from degradation while bound to the Fab molecule. After several months, the initially dark green colour of the rod-shaped crystals of form 1 and the onion-shaped crystals of form 2 faded slowly to light green. Interestingly, when the rod-shaped crystals were investigated after ten months, the green colour of some had changed to a grey-purple colour (compare Figs. 3*e* and 3*f*). This colour is expected when the dye breaks asymmetrically in the linker region, suggesting that in these very old crystals the dye had partially been degraded, but was still bound to the Fab molecule.

It is remarkable that the form 1 crystals grew essentially overnight and very reproducibly, while crystals of forms 2 and 3 were found only after many weeks or even months and initially in only very few drops. Re-checking of old crystal trays after many months to a year showed that form 2 crystals had appeared in many drops that had originally contained only the rod-shaped form 1 (Fig. 3*d*). This may indicate that the growth of form 1 is kinetically favourable while form 2 may be the thermodynamically more stable form.

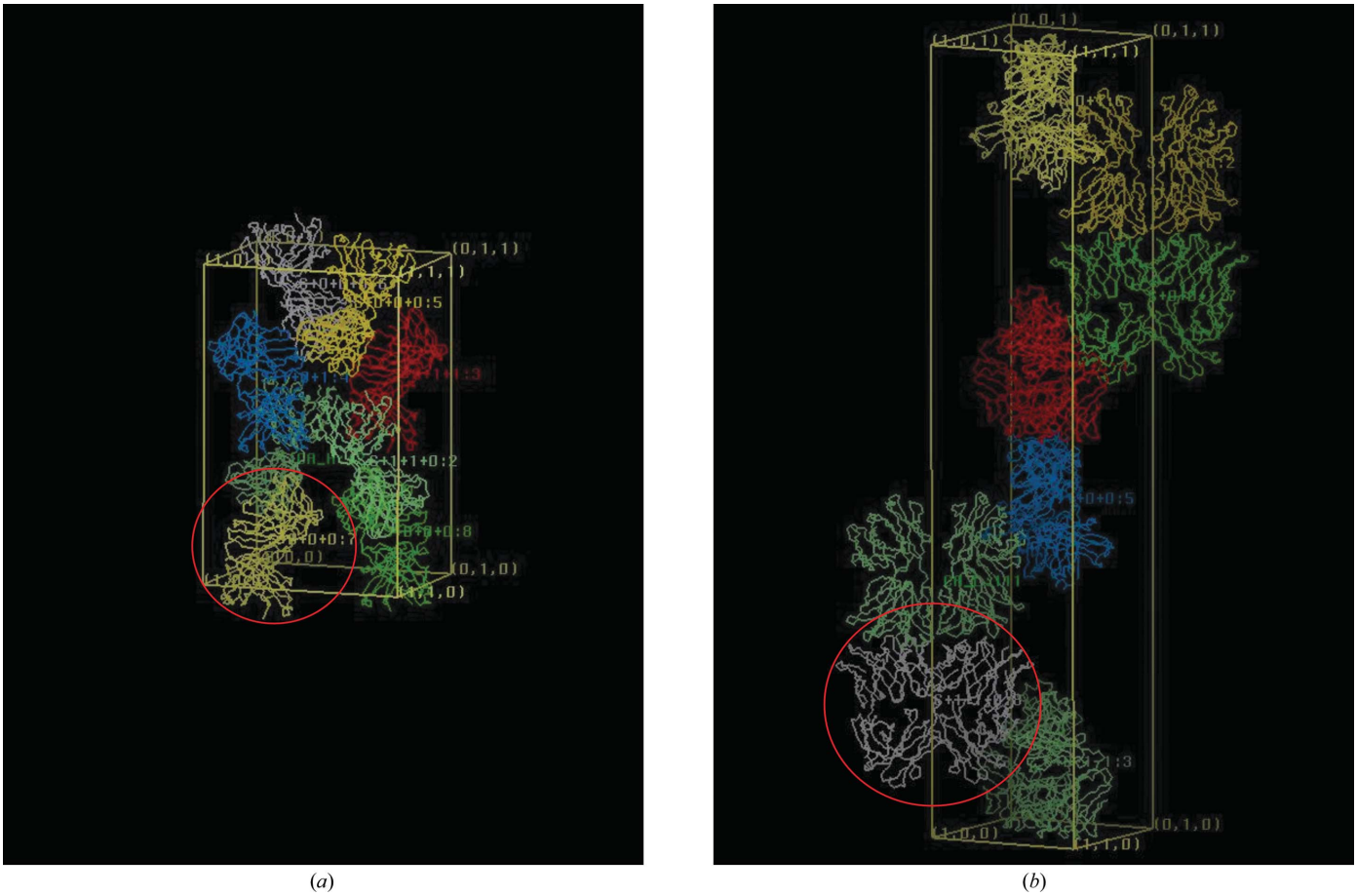

(*a*) (*b*)

Figure 5
Crystal packing. (*a*) C^{α}-filled unit cell of crystal form 1, space group *I*222. (*b*) The same representation for crystal form 2, space group $P4_32_12$. The red circles indicate the Fab monomer and dimer in the asymmetric units of crystal forms 1 and 2, respectively.

3.3. Structure determination and preliminary refinement

Diffraction data could be collected from crystal forms 1 and 2 (Fig. 4). The orthorhombic crystal form 1 belongs to space group *I*222 and contains one Fab molecule per asymmetric unit. A small rod-shaped crystal first diffracted to 3.0 Å at the SLS. A thicker crystal was subsequently used to obtain 2.8 Å data at the BESSY synchrotron. Crystal form 2 belongs to the tetragonal space group $P4_32_12$, with two Fab molecules in the asymmetric unit. For this form, an initial data set to 3.2 Å was collected at BESSY. A second crystal of comparable size later diffracted to 2.85 Å using the stronger SLS source. At 379 Å, the *c* axis of crystal form 2 was extremely long (Figs. 4*b* and 5*b*). The very close reflections in the direction of the *c* axis could be resolved on the diffraction images (Fig. 4*b*), but the required long crystal-to-detector distance resulted in a resolution cutoff at 2.85 Å.

The structures were initially solved for both forms and rebuilding and refinement was initiated using a low-resolution data set (3.0 and 3.2 Å, respectively; data sets 1 and 3 in Table 1). Refinement was later continued using data sets collected to higher resolution (2.80 and 2.85 Å; data sets 2 and 4 in Table 1). A Fab antibody fragment is constituted of the light chain (LC) and a truncated section of the heavy chain (HC). This heavy-chain section has about the same length as the light chain and both the LC and HC fold into an N-terminal and a C-terminal immunoglobulin (Ig) domain. For both chains, the N-terminal Ig domain contains the variable complementarity-determining regions (CDRs) which bind the antigen. This first Ig domain is therefore termed V_L and V_H for the LC and HC, respectively. The second Ig domain is termed the constant region (C_L and C_H1 for the respective chains). In the case of MOR03268, LC and HC are not linked by a disulfide bond. Molecular replacement worked for crystal form 1, conducting separate searches first with a search model for the complete HC and subsequently with a model for the constant region of the light chain (C_L). The orientation of the variable region of the light chain (V_L) was finally found by manually positioning the search model and subsequent rigid-body refinement. The preliminarily refined and rebuilt model of this Fab molecule in crystal form 1 was then used as a search model for form 2.

The crystal packing of the molecular-replacement solutions is shown in Fig. 5. The two Fab molecules in the asymmetric unit of form 2 pack side by side (red circle). Each forms a second Fab dimer with one of its crystallographic symmetry mates, where the coordination is head to head. This arrangement results in a very elongated overall molecular shape. These elongated Fab dimers pack parallel to the very long *c* axis. For both forms difference density for the ligand was found in the region of the antigen-binding site formed by the three CDR loops of each Fab molecule. The TSC dye was placed in the density. Completion of refinement and structure analysis is currently ongoing.

4. Summary

The complex of Fab antibody fragment MOR03268 and its hapten antigen, the green fluorescent dye TSC, was crystallized and data sets were collected from two different crystal forms. A third form diffracted only weakly and was discarded. The stable green colour of the crystals suggests that binding to the Fab molecule protects the dye from hydrolytic degradation. Both crystal forms could be solved by molecular replacement and refinement has been started. Despite the medium to low resolution of the collected data sets, there is difference density at the CDR loops of both forms which fits the expected TSC molecule (data not shown). Refinement and structure analysis is in progress and will be published elsewhere. The structures should reveal the molecular basis of the observed high-affinity recognition of the TSC molecule by MOR03268.

We would like to thank Mira Schmied and Gisela Hübner-Kosney for excellent technical assistance, Marcel Zocher for support during antibody generation, Guido Malawski for help with protein characterization, Martina Schäfer and the beamline staff at BESSY and at SLS for their help during data collection and Ursula Egner and Peter Donner for support.

References

Berman, H. M., Westbrook, J., Feng, Z., Gilliland, G., Bhat, T. N., Weissig, H., Shindyalov, I. N. & Bourne, P. E. (2000). *Nucleic Acids Res.* **28**, 235–242.
Brünger, A. T., Adams, P. D., Clore, G. M., DeLano, W. L., Gros, P., Grosse-Kunstleve, R. W., Jiang, J.-S., Kuszewski, J., Nilges, M., Pannu, N. S., Read, R. J., Rice, L. M., Simonson, T. & Warren, G. L. (1998). *Acta Cryst.* D**54**, 905–921.
Collaborative Computational Project, Number 4 (1994). *Acta Cryst.* D**50**, 760–763.
Gruaz-Guyon, A., Raguin, O. & Barbet, J. (2005). *Curr. Med. Chem.* **12**, 319–338.
Haenel, C., Satzger, M., Della Ducata, D., Ostendorp, R. & Brocks, B. (2005). *Anal. Biochem.* **339**, 182–184.
Kretzschmar, T. & von Rüden, T. (2002). *Curr. Opin. Biotechnol.* **13**, 598–602.
Licha, K. & Perlitz, C. (2004). Patent application WO2004/065491.
Matthews, B. W. (1968). *J. Mol. Biol.* **33**, 491–497.
Ostendorp, R., Frisch, C. & Urban, M. (2004). *Antibodies*, Vol. 2, *Novel Technologies and Therapeutic Use*, edited by G. Subramanian. New York: Kluwer Academic/Plenum Publishers.
Otwinowski, Z. & Minor, W. (1997). *Methods Enzymol.* **276**, 307–326.
Perlitz, C., Licha, K., Scholle, F. D., Ebert, B., Bahner, M., Hauff, P., Moesta, K. T. & Schirner, M. (2005). *J. Fluoresc.* **15**, 443–454.
Rauchenberger, R., Borges, E., Thomassen-Wolf, E., Rom, E., Adar, R., Yaniv, Y., Malka, M., Chumakov, I., Kotzer, S., Resnitzky, D., Knappik, A., Reiffert, S., Prassler, J., Jury, K., Waldherr, D., Bauer, S., Kretzschmar, T., Yayon, A. & Rothe, C. (2003). *J. Biol. Chem.* **278**, 38194–38205.
Vagin, A. & Teplyakov, A. (1997). *J. Appl. Cryst.* **30**, 1022–1025.
Virnekäs, B., Ge, L., Plückthun, A., Schneider, K. C., Wellnhofer, G. & Moroney, S. E. (1994). *Nucleic Acids Res.* **22**, 5600–5607.